Original Article
CASZ1 is a novel promoter of metastasis in ovarian cancer

Yi-Ying Wu[1], Chia-Lin Chang[1], Yuan-Jhe Chuang[1], Jia-En Wu[2], Chia-Hao Tung[2], Yeong-Chang Chen[3], Yuh-Ling Chen[4], Tse-Ming Hong[1], Keng-Fu Hsu[1,3]

[1]Graduate Institute of Clinical Medicine, [2]Institute of Basic Medical Sciences, [3]Department of Obstetrics and Gynecology, National Cheng Kung University Hospital, [4]Institute of Oral Medicine, College of Medicine, National Cheng Kung University, Tainan, Taiwan

Abstract: Epithelial ovarian cancer (EOC) carries the highest mortality rate of all gynecologic malignancies. This high mortality rate is attributed to the fact that most cases of ovarian cancer are detected at late stages when metastases are already present. Through microarray analysis, we previously demonstrated that castor zinc finger 1 (CASZ1) is up-regulated in EOC cells. In contrast to its role in EOC, CASZ1 functions a tumor suppressor in neuroblastoma. Human CASZ1 is predominantly expressed in 2 alternatively spliced isoforms: CASZ1a and CASZ1b. In the present study, we investigated the role of CASZ1 in ovarian cancer cell migration and invasion and assessed the value of CASZ1 expression as a prognostic indicator of metastasis in human ovarian cancer. We used a lentivirus expressing CASZ1-shRNA and a plasmid expressing CASZ1 from a CMV promoter to knockdown and overexpress CASZ1, respectively, in the MCAS, RMUG-S, TOV21G, and A2780^{CP70} ovarian cancer cell lines. mRNA expression levels in tumor tissues and cell lines were measured using quantitative real-time PCR, and CASZ1 protein expression in EOC and paired metastatic tumor tissues was analyzed using immunohistochemistry. We found that CASZ1 was highly expressed in EOC tissues and ovarian cancer cell lines and that CASZ1 knockdown suppressed cell migration and invasion in EOC cells. CASZ1a and CASZ1b exerted similar effects on cell migration and invasion in EOC cells. In addition, CASZ1 promoted the epithelial-mesenchymal transition in EOC cells, and CASZ1 knockdown suppressed cancer metastasis in vivo. Furthermore, CASZ1 protein levels were elevated in human metastatic ovarian tumor tissues. Together, these results indicate that CASZ1 is a novel promoter of EOC metastasis and is highly up-regulated in metastatic EOC tumors.

Keywords: CASZ1, epithelial ovarian cancer, cancer metastasis

Introduction

Epithelial ovarian cancer (EOC) is the most lethal gynecological malignancy [1, 2]. This high lethality is attributed to the fact that the early stage of the disease is mostly asymptomatic; therefore, the disease often remains undiagnosed until the cancer has already disseminated throughout the peritoneal cavity [3]. When EOC is diagnosed at an early stage, prior to metastatic dissemination, the overall 5-year survival rate is approximately 80 to 90%. However, in the approximately 80% of women who are diagnosed after metastases are already present, the survival rate decreases to less than 30%. Metastases are most commonly found within the omentum, the peritoneum, the diaphragm, and the bowel surfaces [4]. As mortality in EOC is directly associated with metastatic disease, ovarian cancer metastasis merits further investigation.

Using a microarray-based analysis, we identified castor zinc finger 1 (CASZ1) as a gene that is up-regulated in EOC. CASZ1, which localizes to chromosome 1p36.22, is the human homolog of the Drosophila zinc finger transcription factor Castor (dCas) [5]. dCas regulates neuronal differentiation and neural fate [6, 7]. In Xenopus laevis and mouse, CASZ1 regulates heart development, cardiomyocyte differentiation, and cardiovascular development [8-11]. Recently, CASZ1 was recognized as a tumor suppressor in neuroblastoma due to its ability

to induce cell differentiation and inhibit tumor cell migration and growth *in vitro* and *in vivo* [12, 13]. Human *CASZ1* localizes to the nucleus and is primarily expressed in 2 alternatively spliced isoforms: CASZ1a and CASZ1b [5]. CASZ1a is a 1,759 amino acid protein composed of 11 zinc fingers. CASZ1b is a 1,166 amino acid protein composed of 5 zinc fingers, and the first 1,166 amino acids of CASZ1b are identical to the sequence of the CASZ1a protein. CASZ1a and CASZ1b exert redundant effects in neuroblastoma [12]. However, the role of CASZ1 in other cancers, including ovarian cancer, remains unclear.

In the present study, we demonstrated that CASZ1 expression is up-regulated in EOC and that CASZ1 promotes EOC metastasis. Furthermore, both CASZ1a and CASZ1b promoted the epithelial-mesenchymal transition (EMT), cell migration, invasion, and metastasis in EOC.

Materials and methods

Cell culture and transfection

The human EOC cell lines, TOV-21G and A2780, were obtained from the American Type Culture Collection (ATCC) (Manassas, VA). The MCAS and RMUG-S cell lines were purchased from the Human Science Research Resources Bank (HSRRB) (Osaka, Japan). TOV-21G cells were maintained in MCDB105 and M199 (1:1) media supplemented with 15% fetal bovine serum (FBS) (Invitrogen, Carlsbad, CA). A2780 and A2780^{CP70} cells were maintained in RPMI 1640 medium supplemented with 10% FBS, 0.1 mM non-essential amino acids, and 1 mM sodium pyruvate. MCAS and RMUG-S cells were maintained in minimum essential medium alpha medium supplemented with 10% FBS and Ham's F12 medium with 10% FBS, respectively. The immortalized ovarian epithelial cell line IOSE396 was generated by transformation with the simian virus 40 [14]. The IOSE396 cells were cultured in RPMI 1640 medium supplemented with 10% FBS. All of the cell lines were incubated in a humidified atmosphere with 5% CO_2 at 37°C. The transient expression of CASZ1a and CASZ1b was achieved by transfecting cells with CASZ1a- and CASZ1b-expressing plasmids, respectively, using Lipofectamine^R LTX&PLUS™ reagent (Invitrogen) (A2780^{CP70} cells) or electroporation using the NEON electroporation system (TOV21G cells). Both transfection procedures were performed according to the manufacturer's protocol.

Patient and tumor specimens

EOC patients who underwent cytoreductive surgery between January 2008 and January 2010 at the National Cheng Kung University Hospital (NCKUH) in Tainan, Taiwan were enrolled in this study. Twenty-eight freshly frozen ovarian cancer specimens and 1 normal ovarian surface tissue were evaluated using quantitative real-time PCR analysis. An additional 20 paired primary and metastatic EOC tissue specimens were evaluated using immunohistochemistry staining. The research protocol and consent form were approved by the NCKUH institutional review board of the hospital, and written informed consent was obtained from each patient.

Quantitative real-time polymerase chain reaction (qRT-PCR)

Total RNA was prepared using the RNeasy Mini Kit (Qiagen, Valencia, CA). One microgram of isolated total RNA was reverse transcribed for 2 h at 42°C using M-MLV Reverse Transcriptase and Oligo(dT)$_{15}$ primers in the presence of an RNase inhibitor (Promega, San Luis Obispo, CA). CASZ1a, CASZ1b, and β-actin mRNA expression levels were measured using qRT-PCR with the Fast SYBR Green Master Mix and the Applied Biosystems StepOne Real-Time PCR System (Applied Biosystems, Foster City, CA) according to the manufacturer's protocol. The resulting cDNA (1:10 dilution) was used as the template for PCR. The 10 μl PCR reaction volume contained 1 μl of cDNA, 0.2 μM forward primer, 0.2 μM reverse primer, and 1x Fast SYBR Green Master Mix. The reaction was conducted using the following PCR conditions: 1) pre-incubation at 95°C for 2 min and 2) 40 cycles of a denaturing step at 95°C for 3 sec and an annealing/extension step at 60°C for 30 sec. The primer sequences were as follows: CASZ1a Forward, 5'-GGATGCTGAGACAGATGAG-TGC-3' and CASZ1a Reverse, 5'-CTGTCGGCA-TAGAGATGGTGTT-3'; CASZ1b Forward, 5'-TCCC-TCCGAGCCTCCGTAT-3' and CASZ1b Reverse, 5'-GGGTCCCTTCCACCCAAGA-3'; and β-actin Forward, 5'-GCCAACCGCGAGAAGATGA-3' and β-actin Reverse, 5'-CATCACGATGCCAGTGGTA-3'. The expression levels of CASZ1a or CASZ1b

were normalized to the expression of β-actin, and relative expression levels were calculated using the following formula: $-\Delta CT = -[CT_{CASZ1a/b} - CT_{\beta-actin}]$. The CASZ1a or CASZ1b cDNA/β-actin cDNA ratio was calculated as $2^{-\Delta CT}$. Relative expression levels of CASZ1a or CASZ1b mRNA are presented as the expression levels in EOC cells compared with normal cells. Control reactions with no template added were included in each assay.

Western blot analysis

The cells were lysed on ice for 30 min in RIPA buffer (0.5% sodium deoxycholate, 0.1% SDS, and 1% Triton X-100 in 1 × TBS) using a stock solution at a 25-fold dilution supplemented with 1 mini protease inhibitor cocktail tablet (Roche Diagnostics, Basel, Switzerland) dissolved in 2 ml of distilled water. Total proteins were separated using SDS-PAGE, transferred to polyvinylidene membranes (Millipore, Billerica, MA) and probed with primary antibodies. The anti-β-actin monoclonal antibody was purchased from GeneTex (San Antonio, TX). The anti-CASZ1 rabbit polyclonal antibody was obtained from Rockland Immunochemicals (Gilbertsville, PA). The anti-E-cadherin and anti-N-cadherin monoclonal antibodies were obtained from BD Biosciences (San Jose, CA), and the anti-α-smooth muscle actin (α-SMA) monoclonal antibody was purchased from Abcam (Cambridge, MA). The antibodies were diluted in TBS (pH 7.5) supplemented with 0.05% (v/v) Tween 20 and 2% bovine serum albumin (BSA). The membranes were incubated with the appropriate horseradish peroxidase-conjugated secondary antibodies (GE Healthcare Life Sciences, Piscataway, NJ), and the bound antibodies were visualized using ECL staining.

CASZ1 knockdown and selection of stable clones

The CASZ1-shRNA-expressing lentiviral vectors were obtained from the National RNAi Core Facility (Academia Sinica, Taipei, Taiwan) and prepared according to standard protocols. The target sequences of sh-CASZ1 (2) and sh-CASZ1 (3) are CGTCACTGAAGATGTAAACAT and CGGCTGCACATTCACTTTCAA, respectively. Briefly, HEK293T cells were co-transfected with pLKO.1 shRNA, pCMV-R8.91, and pMD.G. Virus-containing medium was collected 24 h post-transfection. To generate stably trans-duced shRNA clones, MCAS or RMUG-S cells were infected with the shRNA-expressing lentivirus [multiplicity of infection (MOI) = 3] in media supplemented with 8 μg/ml Polybrene. Twenty-four hours post-infection, the cells were treated with puromycin to select for puromycin-resistant clones.

Wound healing assay

The cells were seeded on ibidi culture inserts (ibidi GmbH, Munich, Germany). After the cells had formed a monolayer, a wound was created by removing the insert. Cell migration was observed, and the cells were imaged at 0 h and at the indicated time points following the creation of the wound. The wound area was measured using ImageJ software (NIH, Bethesda, MD), and the wound area at the indicated time points was normalized to the wound area at 0 h.

Transwell migration assay and in vitro transwell invasion assay

The transwell migration assay and invasion assays were conducted using an 8-μm pore transwell (Corning Costar, Cambridge, MA) coated without or with 100 μg of Matrigel (BD, San Jose, CA). The cells were suspended in media supplemented with 1% FBS and placed in the upper well of the chamber. The lower chamber was filled with media supplemented with 20% FBS. After incubating the cells for the indicated period of time, the cells on the membrane of the transwell were fixed in methanol and stained with Giemsa's solution. The cells attached to the upper surface of the membrane were removed using a cotton swab. Migrating and invasive cells were counted under a light microscope (100 × magnification).

Anchorage-independent growth assay

EOC cells (2×10^4) were seeded in triplicate in media with 0.35% agarose in 6-well plates coated with 0.7% agarose. Anchorage-independent growth was assayed after a 4-week incubation period in complete media, which was replaced every 3 days. The colonies were subsequently stained with 0.25% crystal violet in 20% methanol. After carefully removing the crystal violet solution and rinsing the colonies with water, the colonies were imaged and counted under an inverted microscope.
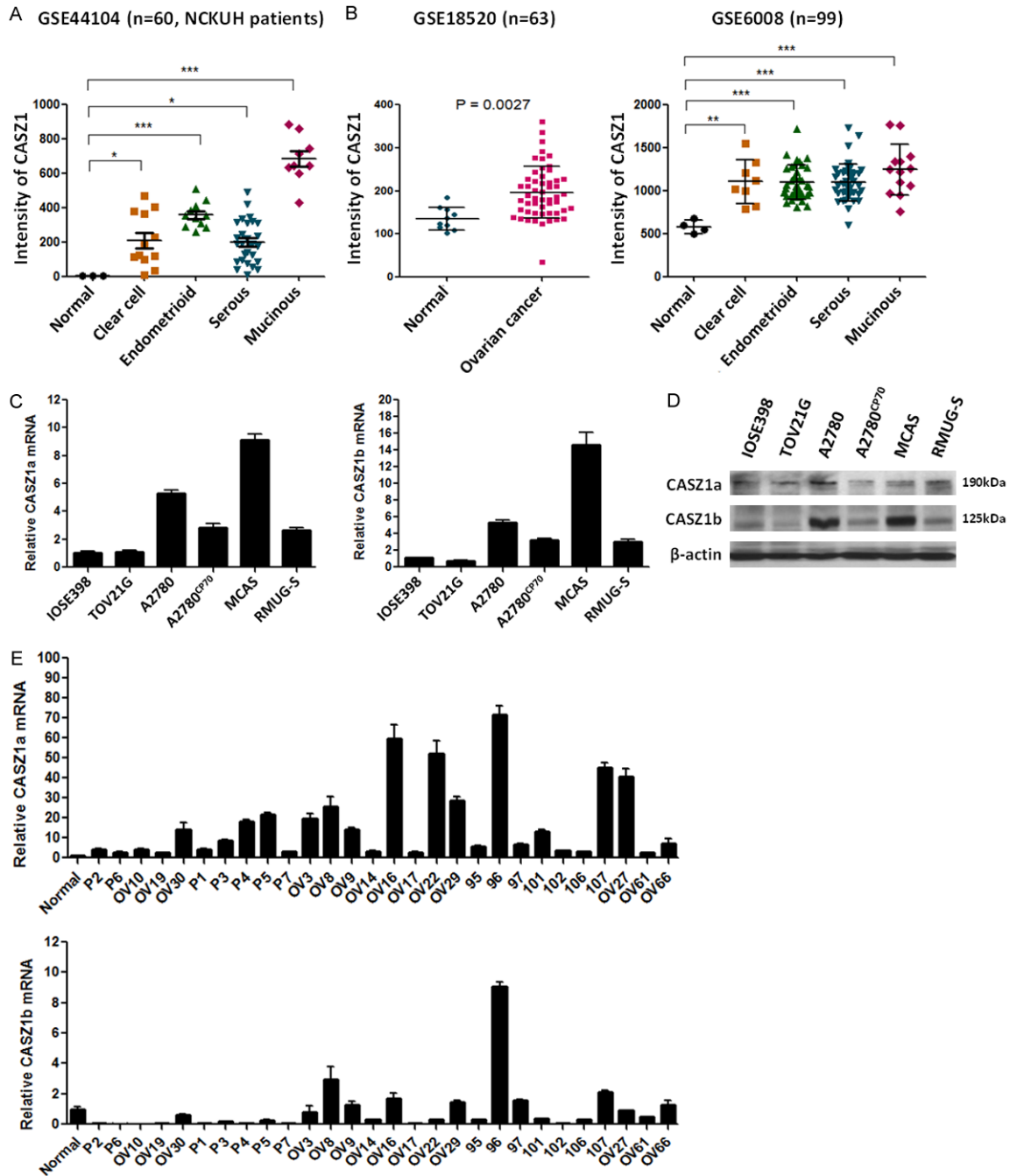
Figure 1. CASZ1 is highly expressed in EOC tissues and EOC cell lines. (A, B) CASZ1 mRNA expression levels were evaluated in clinical EOC specimens using the (A) Affymetrix GeneChip HG-U133_Plus_2 (GSE44104), which included 3 normal ovarian tissues, 12 clear cell, 11 endometrioid, 28 serous, and 9 mucinous ovarian cancer tissues, and (B) 2 GEO databases (GSE6008 and GSE18520). CASZ1 expression levels in the experimental groups and the normal group were compared using Student's t-test. *$P < 0.05$; **$P < 0.005$; ***$P < 0.001$. (C) CASZ1a and CASZ1b mRNA expression levels in human EOC cell lines were determined using qRT-PCR. CASZ1a and CASZ1b expression was normalized to β-actin expression and to CASZ1 expression in IOSE398 cells (an immortalized human ovarian surface epithelial cell line). The qRT-PCR data presented represent 3 independent experiments. (D) CASZ1a and CASZ1b protein levels in human EOC cell lines were determined using immunoblotting assays. β-actin was used as the internal control. (E) CASZ1a and CASZ1b expression in a normal ovarian tissue and tumor tissues derived from 28 EOC patients was assessed using qRT-PCR. The relative level of CASZ1 expression was normalized to β-actin levels and to CASZ1 levels in the normal tissue samples. The error bars represent the SEM.
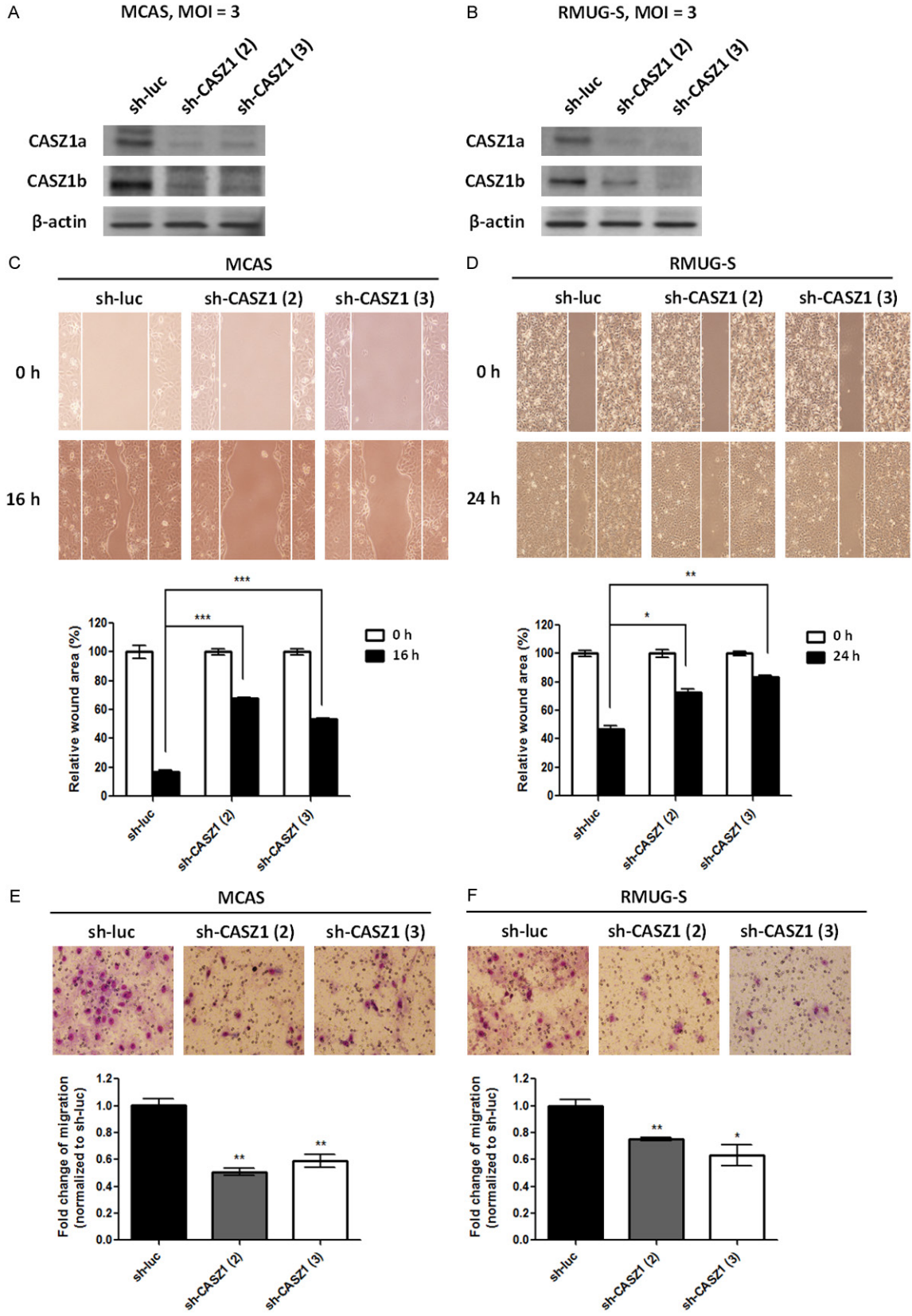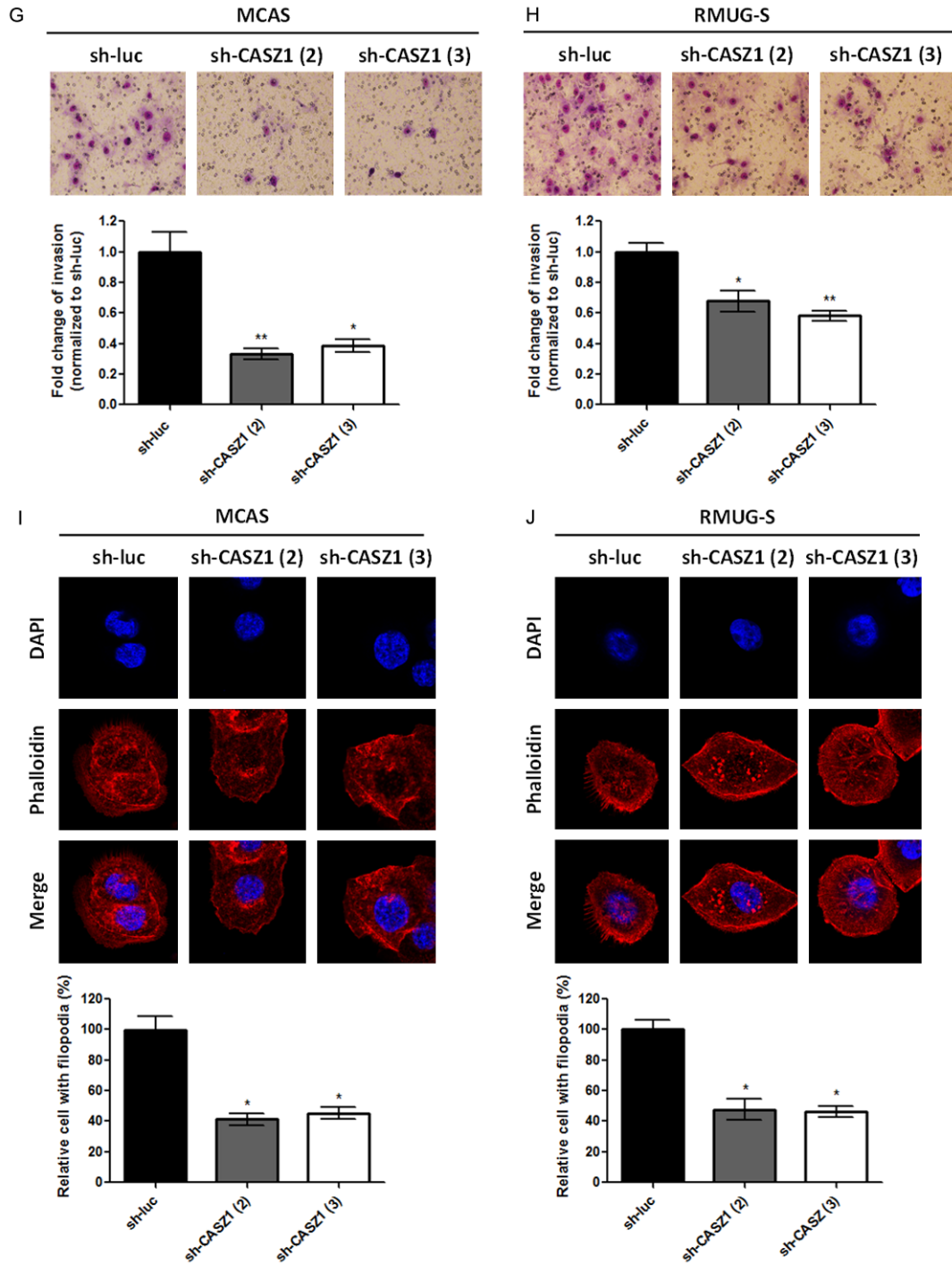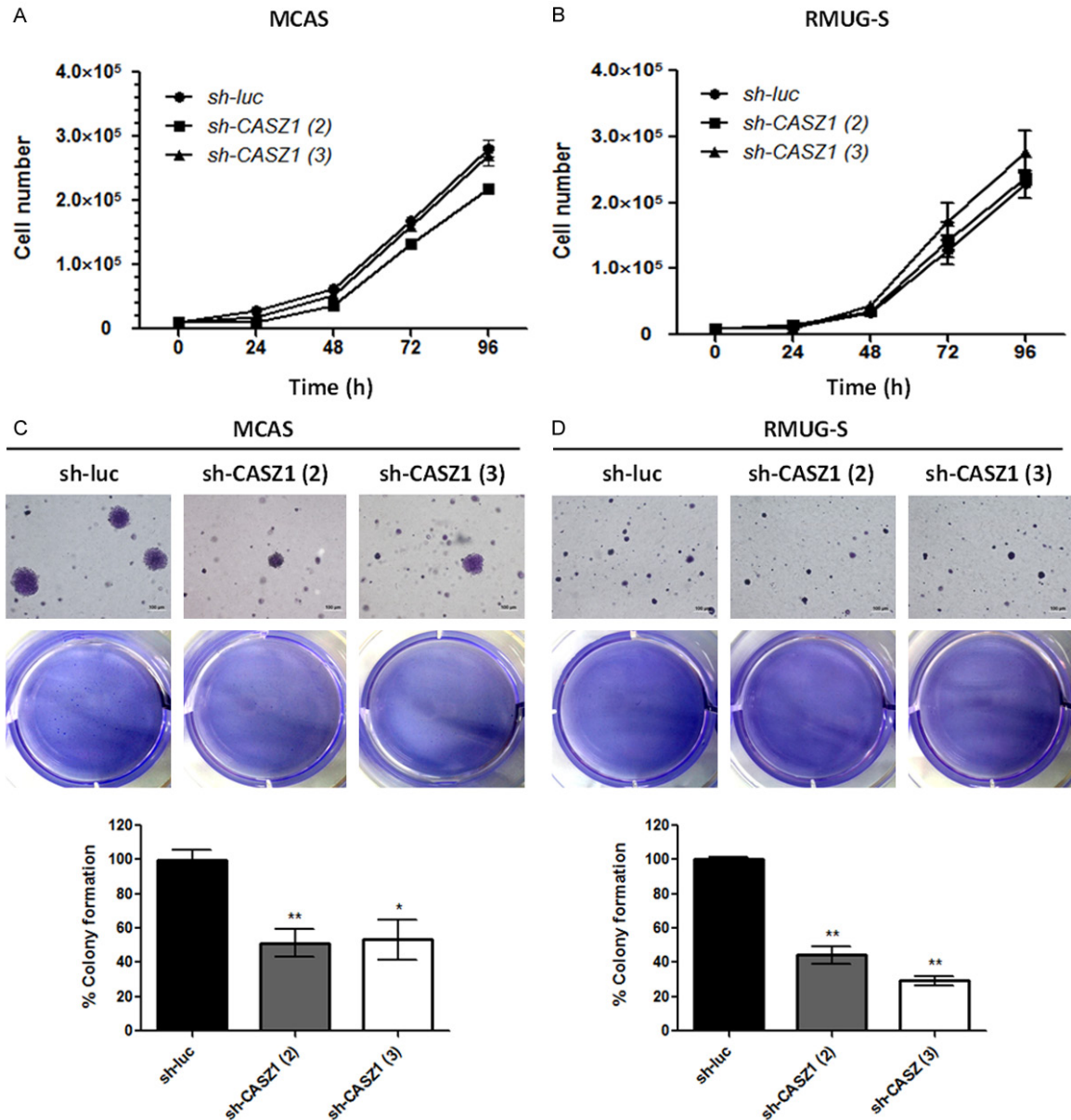
Figure 2. CASZ1 knockdown suppresses migration and invasion in EOC cell lines. MCAS (A, C, E, G, I) and RMUG-S (B, D, F, H, J) cells were infected with the control shRNA (sh-luc) lentivirus or 2 different sh-CASZ1 lentiviruses, and stable clones were selected using puromycin. (A, B) The expression of CASZ1a and CASZ1b in the stable clones was analyzed using immunoblotting assays. β-actin was used as the internal control. The effect of sh-CASZ1 on tumor cell migration was determined using the wound healing assay (C, D) and the transwell migration assay (E, F). For the wound healing assay, 2×10^4 cells expressing sh-luc, sh-CASZ1 (2), or sh-CASZ1 (3) were seeded on ibidi culture inserts. The wound area at 0 h and 16 or 24 h after the removal of culture inserts was measured using ImageJ (n ≥ 3 per group). The wound area at 16 or 24 h was normalized to the wound area measured at 0 h. For the transwell migration assay, 1×10^5 cells expressing sh-luc, sh-CASZ1 (2), or sh-CASZ1 (3) were seeded on the transwells and incubated for 14 h. The cells that had migrated through the transwell were counted (n = 3 per group), and the values were normalized to the sh-luc group to calculate relative migration ability. (G, H) The effect of sh-CASZ1 on tumor

cell invasion was determined using the *in vitro* transwell invasion assay. Briefly, 5 × 10⁵ cells expressing sh-luc, sh-CASZ1 (2), or sh-CASZ1 (3) were seeded on transwells coated with 100 μg of Matrigel and incubated for 24 h. The cells that had invaded the membrane were counted (n = 3 per group), and the values were normalized to the sh-luc group to calculate relative invasive ability. (I, J) CASZ1 knockdown inhibits filopodium formation in EOC cells. Cells were stained with rhodamine phalloidin to visualize F-actin, and the stained cells were observed using confocal microscopy. The number of filopodia-positive cells among a total of 250 cells was counted. The data were normalized to the sh-luc group to calculate the relative number of cells with filopodia. The data represent 3 independent experiments. The error bars represent the SEM. *P < 0.05; **P < 0.005; ***P < 0.001 by Student's t-test.

Figure 3. CASZ1 knockdown does not affect cell proliferation but suppresses anchorage-independent growth in EOC cells. (A, B) The effect of CASZ1 knockdown on EOC cell proliferation. MCAS (A) and RMUG-S (B) cells (1 × 10⁴) expressing sh-luc, sh-CASZ1 (2), or sh-CASZ1 (3) were seeded in 12-well plates and incubated for 4 days. The number of cells was counted each day. Each data point represents the mean ± SEM of 3 wells. (C, D) The effect of CASZ1 knockdown on anchorage-independent growth in MCAS (C) and RMUG-S cells (D). Briefly, 2 × 10⁴ of the indicated cells were plated in soft agar, incubated for 4 weeks, and then stained with 0.01% crystal violet. The number of visible colonies was counted. The data were normalized to the sh-luc group and expressed as the mean ± SEM of 3 wells. *P < 0.05; **P < 0.005 by Student's t-test.
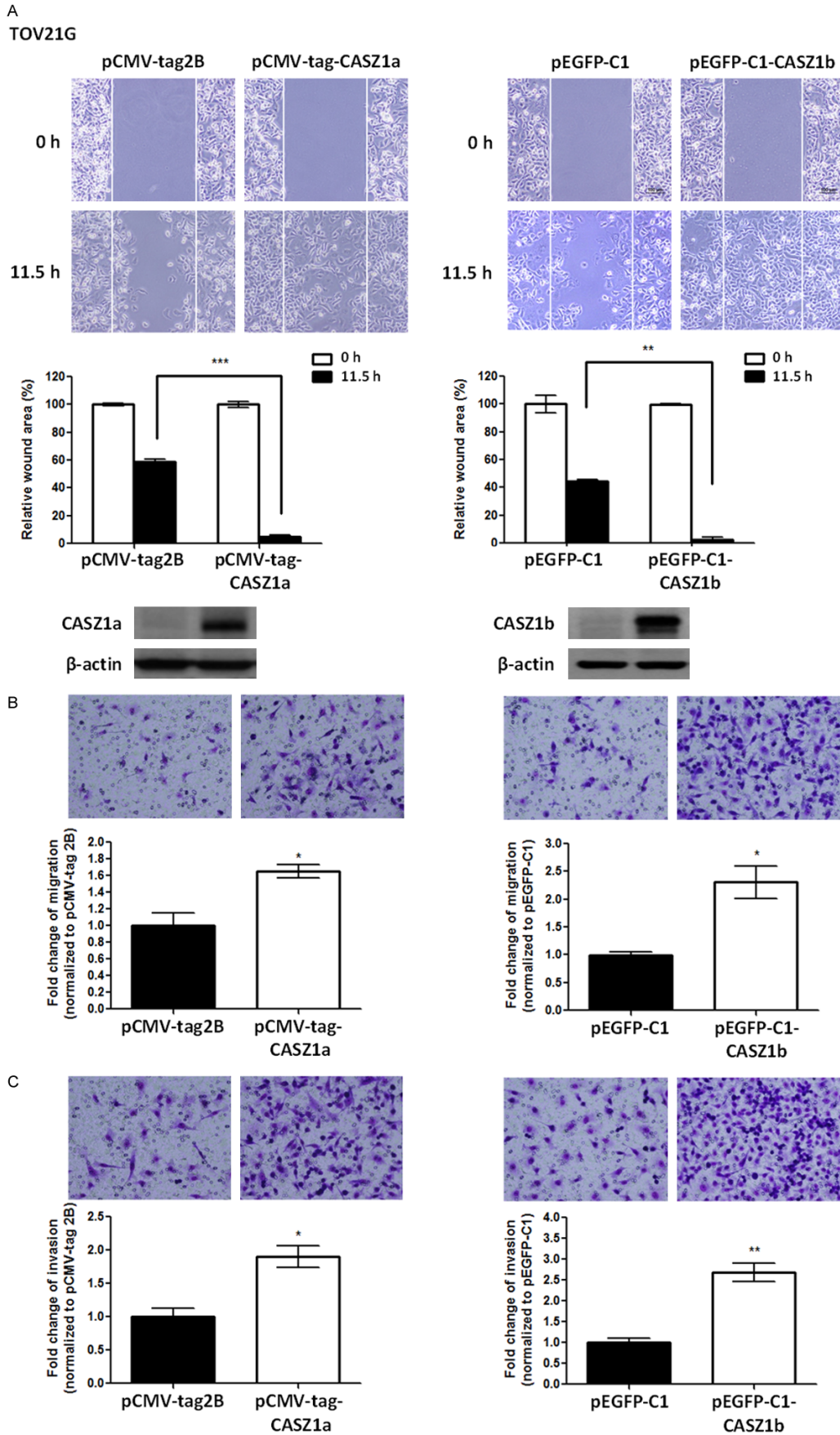
Figure 4. Overexpression of either CASZ1a or CASZ1b enhances migration and invasion in TOV21G cells. A. Both CASZ1a and CASZ1b promote cell migration in TOV21G cells, as demonstrated by the wound healing assay. TOV21G cells were electroporated with the pCMV-tag2B, pCMA-tag-CASZ1a (left panel), pEGFP-C1 vector, or pEGFP-C1-CASZ1b vector (right panel). Twenty-four hours later, 2×10^4 of the indicated cells were seeded on ibidi culture inserts. The wound was imaged (upper panel) at 0 h and 11.5 h after the removal of culture inserts, and the wound area was measured using ImageJ (n ≥ 3 per group). The wound area at 11.5 h was normalized to the wound area at 0 h (middle panel). CASZ1a and CASZ1b expression was analyzed using immunoblotting assays (lower panel). β-actin was used as the internal control. B. Both CASZ1a and CASZ1b promote cell migration in TOV21G cells, as demonstrated using the transwell migration assay. Briefly, 2×10^4 of the indicated cells were seeded on transwells and incubated for 6 h. The cells that had migrated through the transwell were counted (n = 3 per group), and the values were normalized to the vector control group to calculate relative migration ability. C. The effect of CASZ1a or CASZ1b on cell invasion in TOV21G cells was determined using the *in vitro* transwell invasion assay. Briefly, 1×10^5 cells were seeded on transwells coated with 100 μg of Matrigel and incubated for 24 h. The cells that had invaded the membrane were counted (n = 3 per group), and the values were normalized to the vector control group to calculate relative invasive ability. The error bars represent the SEM. *$P < 0.05$; **$P < 0.005$; ***$P < 0.001$ by Student's t-test.

Experimental metastasis in vivo

MCAS cells (5×10^5) transfected with sh-luc or sh-CASZ1 (2) were suspended in 200 μl of Hank's balanced salt solution (HBSS) and injected into 5 8-week-old SCID mice in each group via the lateral tail vein. The injected mice were euthanized 7 weeks later, and their lungs were resected and fixed in 10% formalin. The lung tumor cell colonies were counted under a dissecting microscope. Representative lung tumors were resected, fixed, and embedded in paraffin. The embedded tissue was sectioned into 4-μm sections, and the sections were stained with hematoxylin-eosin (H&E) for histological analysis.

Immunohistochemistry

The tissue sections used for the immunohistochemistry analysis of CASZ1 protein expression were autoclaved in Tris-EDTA buffer (pH 9) at 121°C for 10 min for antigen retrieval. The samples were subsequently treated with 3% H_2O_2-methanol and incubated with the antibody against CASZ1 diluted 1:1,000 in antibody dilution buffer (DakoCytomation Inc., Carpinteria, CA) overnight at 4°C. The immunoreactive staining was visualized using the LSAB+ system-HRP and the AEC substrate (DakoCytomation, Inc.). Then, the samples were counterstained with hematoxylin. CASZ1 expression in the tumor tissues was scored as follows: 0, no CASZ1 expression; 1, 0-25% CASZ1-positive tumor cells; 2, 26-50% CASZ1-positive tumor cells; and 3, 51-100% CASZ1-positive tumor cells.

Statistical analysis

The data are presented as the mean ± standard error of the mean (SEM). Comparisons between 2 groups were calculated using Student's t-test, and comparisons between paired tumor samples were calculated using the Wilcoxon signed-rank test using GraphPad Prism software (Version 5.0). All of the statistical tests were two-sided, and *P*-values <0.05 were considered statistically significant.

Results

CASZ1 is highly expressed in EOC tissues and ovarian cancer cell lines

To identify putative EOC biomarkers and therapeutic targets, we analyzed the global gene expression profiles of ovarian cancer tissues obtained in our previous microarray study (GEO number: GSE44104) [15]. These data demonstrated that CASZ1 was up-regulated in various types of EOC cells, including the clear cell, endometrioid, serous, and mucinous subtypes, compared with normal ovarian tissues (**Figure 1A**). Consistent with these findings, an increase in CASZ1 expression in EOC tissues was reported in other GEO databases, including GSE-18520 and GSE6008 (**Figure 1B**). In mammals, the *CASZ1* gene encodes 2 isoforms: CASZ1a (*hCasz11*), which has 11 zinc fingers, and CASZ1b (*hCasz5*), which has 5 zinc fingers. These genes are co-expressed and have redundant functions in suppressing tumor cell growth in neuroblastoma [12]. Therefore, we analyzed the expression levels of CASZ1a and CASZ1b in EOC cell lines and clinical EOC specimens. With the exception of the TOV21G cells, CASZ1a and CASZ1b mRNA and protein expression levels were elevated in the EOC cell lines (A2780, A2780^CP70, MCAS, and RMUG-S) compared with an immortalized human ovarian surface epithelial cell line (IOSE398) (**Figure 1C** and **1D**). In addition, CASZ1a and CASZ1b were co-
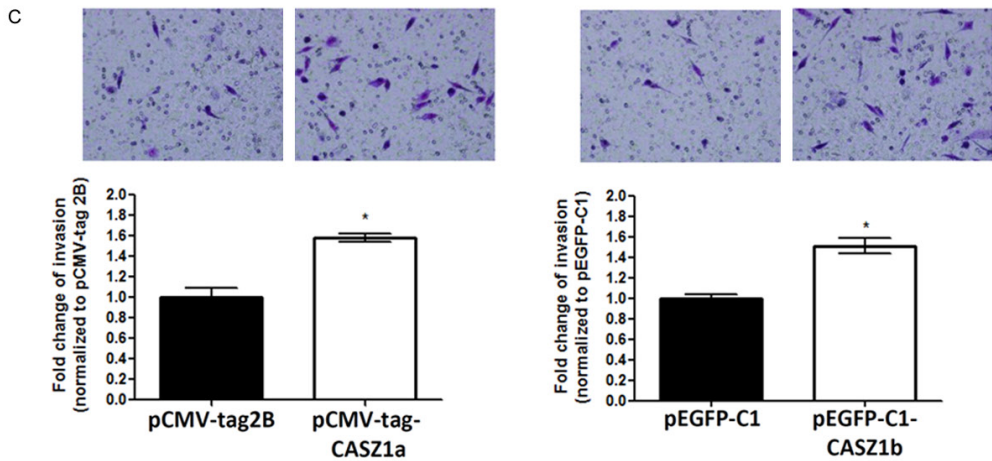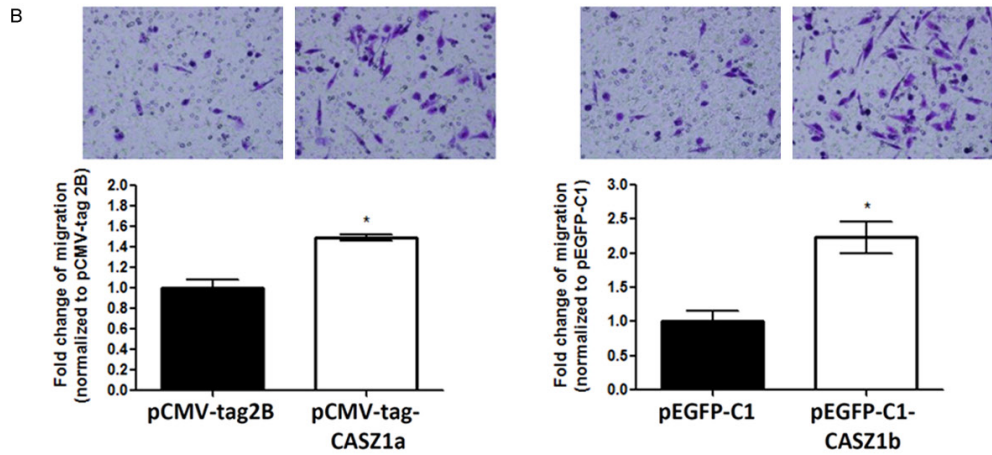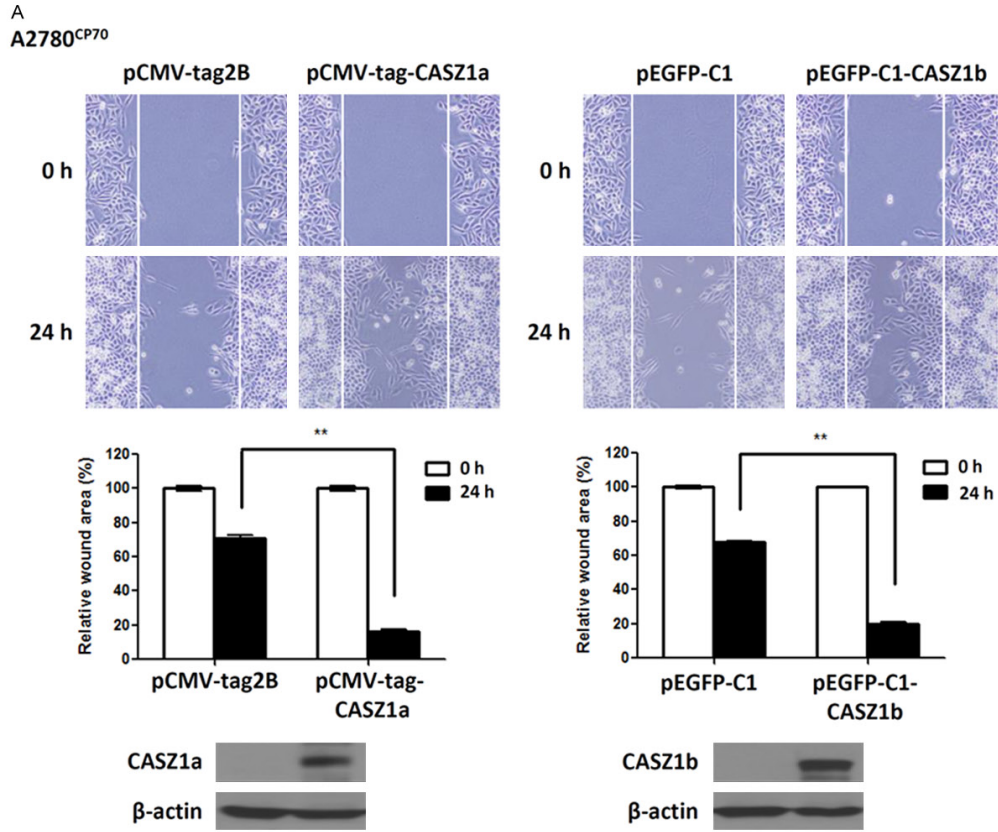
Figure 5. CASZ1a or CASZ1b overexpression enhances cell migration and invasion in A2780^{CP70} cells. A. CASZ1a and CASZ1b promote cell migration in A2780^{CP70} cells, as demonstrated by the wound healing assay. A2780^{CP70} cells were transfected with the pCMV-tag2B, pCMA-tag-CASZ1a (left panel), pEGFP-C1, or pEGFP-C1-CASZ1b vector (right panel). Twenty-four hours later, 2×10^4 of the indicated cells were seeded on ibidi culture inserts. The wound was imaged (upper panel) at 0 h and 24 h after the removal of the culture inserts, and the wound area was measured using ImageJ (n ≥ 3 per group). The wound area at 24 h was normalized to the wound area at 0 h (middle panel). CASZ1a and CASZ1b expression was analyzed using immunoblotting assays (lower panel). β-actin was used as the internal control. B. The effect of CASZ1a or CASZ1b on tumor cell migration in A2780^{CP70} cells was determined using the transwell migration assay. Briefly, 2×10^5 of the indicated cells were seeded on transwells and incubated for 14 h. The cells that had migrated through the transwell were counted (n = 3 per group), and the values were normalized to the vector control group to calculate relative migration ability. C. The effect of CASZ1a and CASZ1b on tumor cell invasion in A2780^{CP70} cells was determined using the *in vitro* transwell invasion assay. Briefly, 2×10^5 cells were seeded on transwells coated with 100 µg of Matrigel and incubated for 24 h. The number of cells that had invaded the membrane was counted (n = 3 per group), and the values were normalized to the vector control group to calculate relative invasive ability. The error bars represent the SEM. *$P < 0.05$; **$P < 0.005$; ***$P < 0.001$ by Student's t-test.

expressed in EOC cell lines. We also assessed CASZ1a and CASZ1b mRNA levels in 28 clinical EOC tumor specimens and 1 normal ovarian tissue specimen using qRT-PCR (**Figure 1E**). CASZ1a expression levels were at least 2-fold greater in all of the EOC clinical specimens compared with the normal tissue, whereas CASZ1b was up-regulated in 9 of the 28 EOC clinical specimens. Compared with CASZ1b, CASZ1a was more frequently and more strongly up-regulated in EOC tissues.

CASZ1 knockdown suppresses cell migration and invasion in EOC cells

To determine the role of CASZ1 in EOC, 2 ovarian cancer cell lines, MCAS and RMUG, were infected with lentiviral-based shRNAs targeting CASZ1 or a control luciferase gene. Cell migration, invasion and proliferation were evaluated in the resulting CASZ1-knockdown EOC cells. CASZ1a and CASZ1b protein levels were efficiently knocked down in MCAS and RMUG-S cells (**Figure 2A** and **2B**). In addition, a wound healing assay (**Figure 2C** and **2D**) and transwell migration assay (**Figure 2E** and **2F**) demonstrated that CASZ1 knockdown inhibited cancer cell migration, and an *in vitro* transwell invasion assay (**Figure 2G** and **2H**) demonstrated that CASZ1 knockdown inhibited cell invasion. Actin cytoskeleton rearrangements are involved in the formation of lamellipodia and filopodia and are vital for cancer cell migration/invasion and the cellular events that mediate metastasis. Therefore, we investigated the influence of CASZ1 knockdown on cytoskeleton assembly in MCAS and RMUG-S cells and found that CASZ1 knockdown reduced the formation of filopodia in MCAS and RMUG-S cells (**Figure 2I**

and **2J**). Although CASZ1 was reported to regulate the expression of several cell growth-associated genes and suppress cell proliferation in neuroblastoma [11], we found that CASZ1 knockdown did not affect proliferation in MCAS and RMUG cells (**Figure 3A** and **3B**). Furthermore, CASZ1 knockdown suppressed anchorage-independent cell growth (**Figure 3C** and **3D**).

CASZ1a and CASZ1b exert similar effects on cell migration and invasion in EOC cells

As the *CASZ1* gene encodes 2 isoforms, CASZ1a and CASZ1b, that are co-expressed in ovarian cancer cells, we overexpressed CASZ1a or CASZ1b in TOV21G cells expressing low levels of CASZ1 to investigate their individual roles in EOC cell motility and invasion. Indeed, overexpression of either CASZ1a or CASZ1b promoted cancer cell motility, as demonstrated by a wound healing assay (**Figure 4A**) and a transwell migration assay (**Figure 4B**). In addition, CASZ1a and CASZ1b overexpression enhanced cell invasion in TOV21G cells (**Figure 4C**). To confirm these findings, we overexpressed CASZ1a or CASZ1b in another ovarian cancer cell line, A2780^{CP70}. Similar to what was observed in TOV21G cells, cell migration and invasion were enhanced in A2780^{CP70} cells overexpressing either CASZ1a or CASZ1b (**Figure 5**).

CASZ1 mediates EMT in EOC cells

We analyzed the expression of various EMT marker genes in CASZ1-overexpressing and CASZ1-knockdown EOC cells. In CASZ1a- or CASZ1b-overexpressing TOV21G and A2780^{CP70} cells, the expression of the mesenchymal mark-
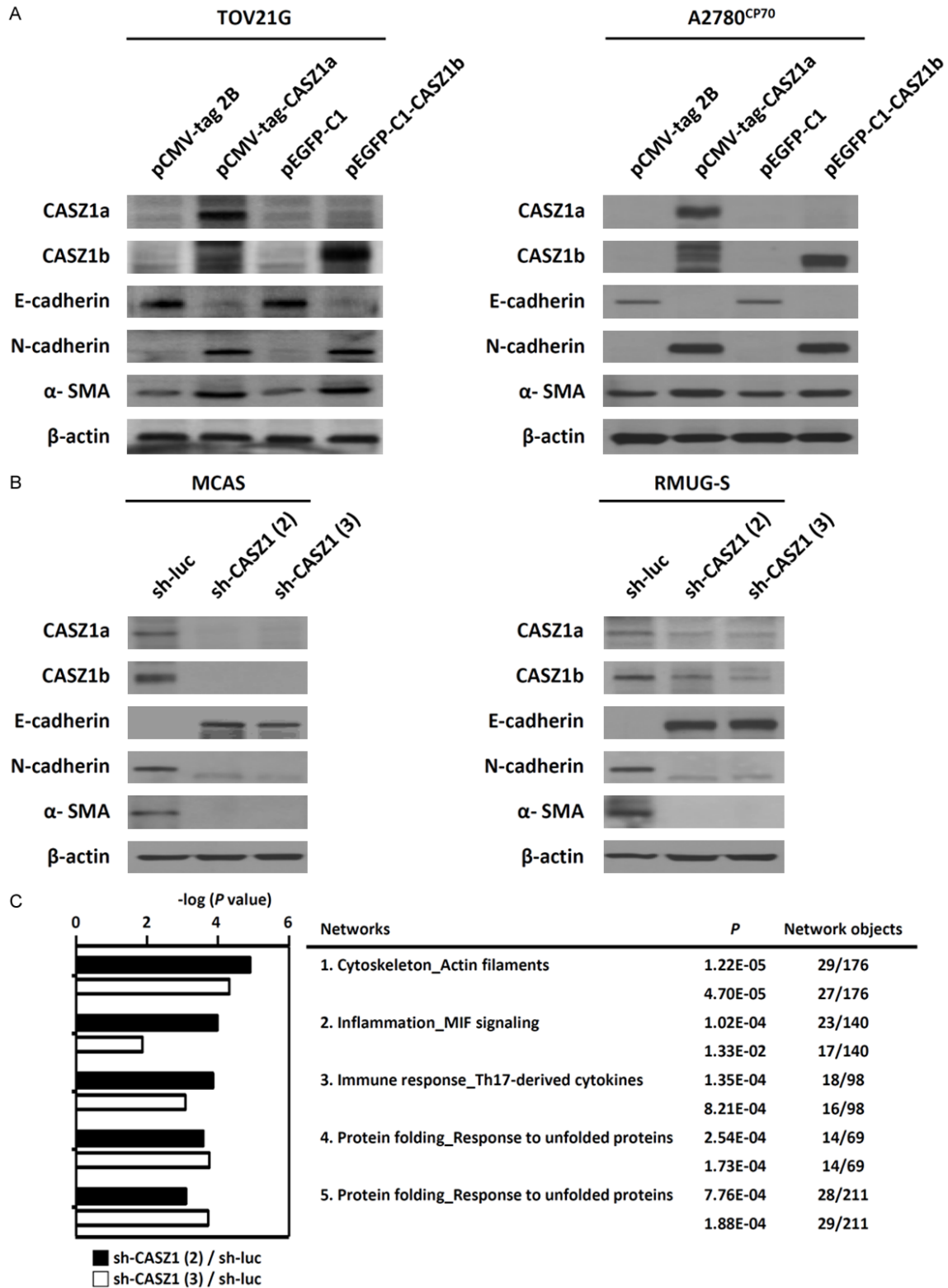
Figure 6. CASZ1 promotes the epithelial-mesenchymal transition and cancer metastasis in EOC cells. Changes in the expression of EMT-associated genes in (A) CASZ1a- or CASZ1b-overexpressing TOV21G and A2780[CP70] cells and in (B) CASZ1-knockdown MCAS and RMUG cells were analyzed using immunoblotting assays. Epithelial marker: E-cadherin; mesenchymal markers: N-cadherin and α-smooth muscle actin (α-SMA). β-actin was used as the internal control. (C) The 5 most highly enriched networks identified by the MetaCore-based analysis of the microarray data derived from MCAS cells expressing sh-luc, sh-CASZ1 (2), and sh-CASZ1 (3).
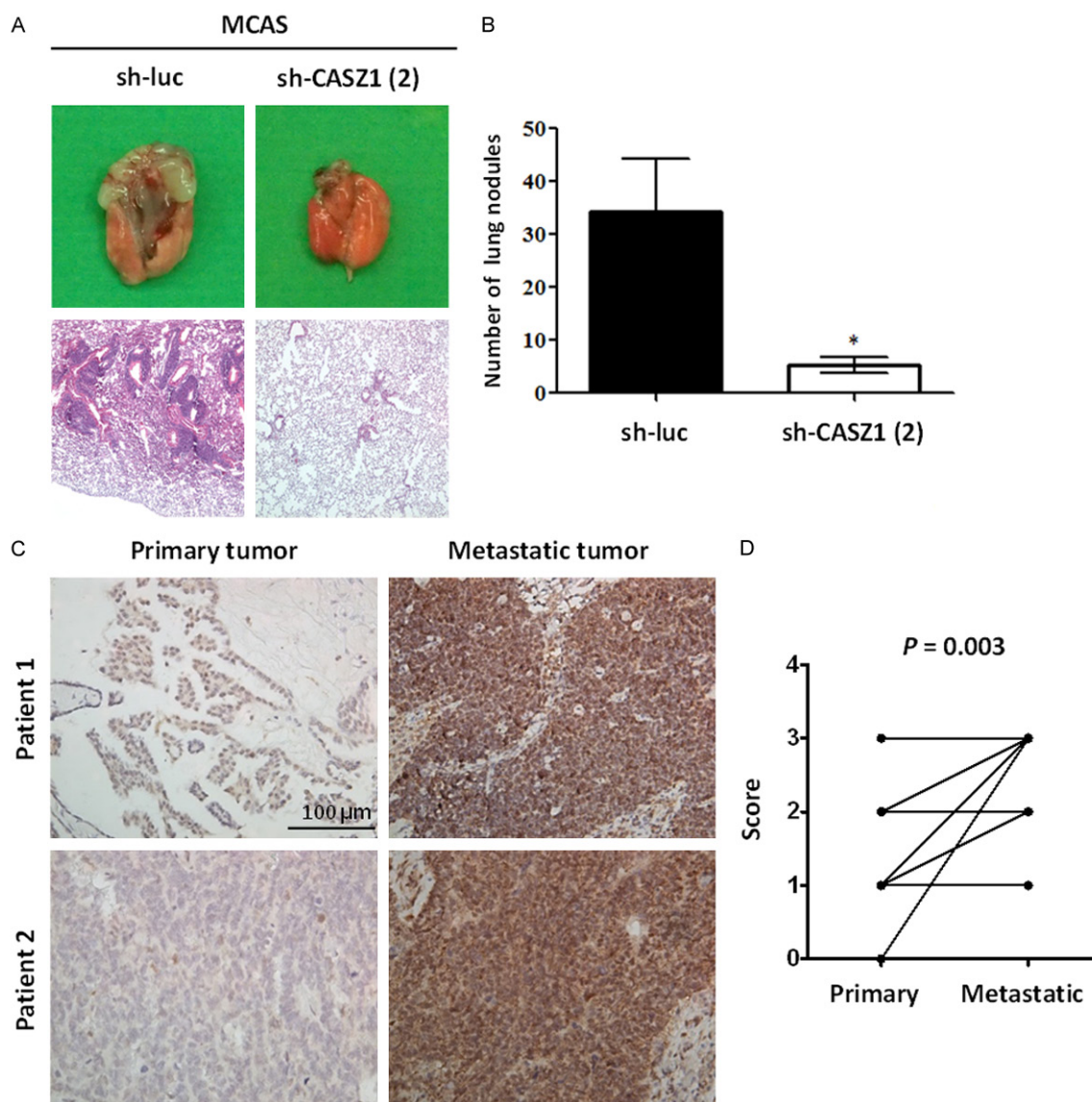
Figure 7. Human metastatic ovarian tumors express high levels of CASZ1. A, B. The effect of CASZ1 knockdown on metastasis *in vivo*. Briefly, 5×10^5 MCAS cells expressing sh-luc or sh-CASZ1 (2) were intravenously injected into mice, and the mice were euthanized 7 weeks after the injection. A. Upper panel: representative image of lungs derived from the mice injected with MCAS cells expressing sh-luc or sh-CASZ1 (2). Lower panel: histological analysis of a mouse lung using H&E staining. B. Quantification of lung metastatic nodules 7 weeks after the injection. The data are expressed as the mean ± SEM. *P = 0.02 by Student's t-test. (n = 5 mice per group). C. Two representative paired ovarian primary and metastatic tumors stained with an antibody against CASZ1. Upper right, para-aortic lymph node; lower right, peritoneal metastatic tumor. Scale bar: 100 μm. D. Samples from a total of 20 EOC patients with stage III or IV disease were evaluated. The paired primary and metastatic tumors were stained with an antibody against CASZ1 and scored according to the following scoring system: 0: no expression, 1: 1-25% CASZ1-positive tumor cells; 2: 26-50% CASZ1-positive tumor cells; and 3: 51-100% CASZ1-positive tumor cells. Among the primary tumor samples, 1 was assigned a score of 0, 14 were assigned a score of 1, 4 were assigned a score of 2, and 1 was assigned a score of 3. Among the metastatic tumor samples, 6 were assigned a score of 1, 4 were assigned a score of 2, and 10 were assigned a score of 3. Compared with the paired primary tumors, CASZ1 expression was significantly up-regulated in the metastatic tumors. P = 0.003 by Wilcoxon signed-rank test.

ers N-cadherin and α-SMA was up-regulated, whereas the expression of the epithelial marker E-cadherin was down-regulated (**Figure 6A**).

Conversely, the expression of E-cadherin was up-regulated in CASZ1-knockdown MCAS and RMUG-S cells, whereas the expression of

Table 1. CASZ1 expression in primary and metastatic tumors from 20 epithelial ovarian cancer patients as determined using immuno-histochemistry staining

	Primary tumor	Metastatic tumor
High CASZ1 expression	1	10
Low CASZ1 expression	19	10
P = 0.0014 by chi-square		

High CASZ1 expression was defined as 50% CASZ1-positive neoplastic cells, and low CASZ1 expression was defined as less than 50% CASZ1-positive neoplastic cells.

N-cadherin and α-SMA was down-regulated (**Figure 6B**). These results indicate that CASZ1 triggers EMT in EOC cells.

To investigate the mechanisms that mediate the effects of CASZ1 on EMT and cancer cell migration/invasion in EOC cells, we used the MetaCore tool to analyze genes identified by the microarray data as up- and down-regulated at least 1.5-fold in CASZ1-silenced MCAS cells compared with control cells. The top 5 networks associated with the differentially expressed genes are presented in **Figure 6C**, and the most highly enriched network identified was "Cytoskeleton_actin filaments." The 10 most highly up- and down-regulated genes are listed in Supplementary Table 1.

CASZ1 knockdown suppresses cancer metastasis in vivo

Based on our *in vitro* data, we postulated that CASZ1 expression is associated with cancer metastasis in EOC. To determine the effect of CASZ1 expression on metastatic colonization, we intravenously injected severe combined immunodeficiency (SCID) mice with CASZ1-knockdown MCAS cells transfected with sh-CASZ1 (2) or control cells transfected with sh-luc. The mice were euthanized 7 weeks after the injections. As shown in **Figure 7A** and **7B**, mice injected with CASZ1 knockdown cells developed significantly fewer lung metastatic nodules compared with mice injected with the control cells. These results indicate that CASZ1 knockdown suppresses the ability of MCAS cells to form metastatic nodules in the lungs.

CASZ1 expression is up-regulated in human metastatic ovarian tumors

To further investigate the metastasis-promoting effects of CASZ1 in EOC, we evaluated

CASZ1 expression in paired primary and metastatic tumors from 20 EOC patients with stage III or stage IV disease using immunohistochemistry. As shown in **Figure 7C**, CASZ1 protein expression was up-regulated in metastatic tumor tissues compared with the paired primary tumor tissues. CASZ1 expression levels were assigned a score from 0 to 3 according to the following scoring system: 0, no expression; 1, 1-25% CASZ1-positive tumor cells; 2, 26-50% CASZ1-positive tumor cells; and 3, 51-100% CASZ1-positive tumor cells. Among the primary tumors, 1 was assigned a score of 0, 14 were assigned a score of 1, 4 were assigned a score of 2, and 1 was assigned a score of 3. Among the metastatic tumors, 6 were assigned a score of 1, 4 were assigned a score of 2, and 10 were assigned a score of 3. Compared with the paired primary tumors, there was a statistically significantly increase in CASZ1 expression in metastatic tumors (P = 0.003 as calculated by Wilcoxon signed-rank test) (**Figure 7D**). Thus, higher CASZ1 expression was associated with metastatic EOC tumor tissues (**Table 1**).

Discussion

In the present study, we demonstrated that CASZ1 is overexpressed in EOC cell lines and tissues and promotes EOC metastasis. Both isoforms of CASZ1, CASZ1a and CASZ1b, promoted EMT and enhanced cancer cell migration and invasion *in vitro* and promoted cancer metastasis *in vivo*. Furthermore, we confirmed that CASZ1 expression is up-regulated in metastatic tumor tissues compared with matched primary tumors derived from patients with metastatic ovarian cancer. Thus, CASZ1 might be involved in EOC metastasis and thus serves as a potential prognostic marker of metastatic EOC.

CASZ1 is a zinc-finger transcription factor that plays a key role in various developmental processes, including neurogenesis, heart development, and vascular morphogenesis [5, 7-11]. The loss of CASZ1 is associated with a poor prognosis in patients with neuroblastoma [12, 13]. In this context, CASZ1 is recognized as a tumor suppressor in neuroblastoma because it promotes cell differentiation and adhesion and inhibits cell proliferation and motility. However, the role of CASZ1 in other types of cancer, such as EOC, remains unclear. We evaluated the association of CASZ1 with EOC progression and found that in contrast to its tumor suppressor

role in neuroblastoma, CASZ1 promotes metastasis in EOC. CASZ1 was up-regulated in EOC tissues, especially in metastatic tumor tissues, and CASZ1 promoted EOC cell migration, invasion, and metastasis. We also analyzed CASZ1 expression in the GSE66934 GEO dataset of gene expression in a mouse metastatic ovarian cancer model (Supplementary Figure 1). CASZ1 expression was up-regulated in highly metastatic ID8-M cells derived from ascites in mice intraperitoneally injected with parental ID8 mouse ovarian epithelial papillary serous adenocarcinoma cells. Consistent with previous reports, we found that the overexpression of CASZ1a or CASZ1b suppressed cell migration in the SH-SY5Y neuroblastoma cell line (Supplementary Figure 2). These findings indicate that CASZ1 might have distinct functions and target genes in ovarian cancer and neuroblastoma tissues. An *in silico* data mining analysis using EST clustering data from the ECgene database (http://genome.ewha.ac.kr/ECgene/) revealed that CASZ1 mRNA was highly expressed in cancer tissues derived from the lung, muscle, ovary, pancreas, large intestine, stomach, and skin, whereas CASZ1 mRNA was down-regulated in prostate and breast cancer tissues (Supplementary Figure 3). Furthermore, the deletion of chromosome 1p36, which harbors the *CASZ1* gene, is frequently observed in several types of cancers, including neuroblastoma, melanoma, and breast cancer [16]. These findings further indicate that CASZ1 might be associated with cancer progression and that CASZ1 plays distinct roles in different types of cancers.

In addition to inhibiting cell migration and invasion, CASZ1 knockdown suppressed anchorage-independent cell growth. However, CASZ1 knockdown did not affect cell proliferation. The effect of CASZ1 on cell proliferation in MCAS and RMUG-S cells is interesting. Although CASZ1 regulates the expression of several cell growth-associated genes and suppresses cell proliferation and anchorage-independent cell growth in neuroblastoma [12, 13], the loss of CASZ1 expression inhibits cell proliferation by inducing cell cycle arrest at the G1/S transition in cardiomyocytes [17] and endothelial cells [11]. We used Ingenuity Pathways Analysis (IPA) to analyze the gene expression profiles of MCAS cells expressing sh-luc, sh-CASZ1 (2), or sh-CASZ1 (3). The first, second and seventh most

highly differentially expressed genes are involved in cell death and survival, cell movement, and cellular growth and proliferation, respectively (Supplementary Figure 4). It is possible that we did not observe an effect on the proliferation of CASZ1-knockdown MCAS and RMUG-S cells during the time frame of our experiments due to their relatively low basal proliferation rate.

Furthermore, we observed a reduction in the expression of several genes associated with EOC progression and malignancy in CASZ1-knockdown MCAS cells, including interleukin-6 (IL-6), IL-8, TNF-α, CXCL1, CXCL2, CCL20, SAA1, SAA2, SAA4, MMP7, and S100A4, using microarray analysis (Supplementary Table 1). Previous studies demonstrated that IL-6 and IL-8 are cytokines that play key roles in EOC progression. Moreover, IL-6 is recognized as a therapeutic target of EOC therapy [18, 19]. IL-6 expression is associated with a poor prognosis and the presence of malignant ascites, and this cytokine plays a central role in tumor growth, angiogenesis, and malignancy in EOC [20-24]. IL-8, the most highly down-regulated gene in CASZ1-knockdown MCAS cells, is associated with a poor prognosis in EOC patients and promotes cell growth, angiogenesis, EMT, migration, and invasion in EOC cells [20, 21, 25-29]. Therefore, in EOC, CASZ1 might trigger EMT, anchorage-independent cell growth, cell migration/invasion, and cancer metastasis via IL-6 and IL-8 signaling. In addition, TNF-α is a prognostic factor in EOC and is associated with EOC immunosuppression [30, 31]. TNF-α promotes a pro-inflammatory tumor microenvironment and induces the expression of several inflammatory chemokines, including CXCL1, CXCL2, and CCL20, via NF-κB activation [32]. These inflammatory chemokines control the recruitment of neutrophils or tumor-derived T_{reg} cells. The recruited cells promote cancer cell immunosuppression and the expression of metastasis-promoting genes associated with cancer migration/invasion [33-35]. Moreover, the blood levels of acute-phase serum amyloid A proteins, including SAA1, -2 and -4, increase during the early stages of various cancers, including EOC, and are overexpressed in EOC [36-38]. The expression of SAA proteins is induced by IL-1, IL-6, and TNF-α, and these proteins stimulate immunosuppressive neutrophils to produce IL-10, thereby suppressing cell

immunity. Furthermore, we found that CASZ1 might regulate the expression of matrix metalloprotease 7 (MMP7) in EOC cells. MMPs play an important role in tumor invasion via their extracellular matrix degradation activity. Indeed, MMP7 may serve as a valuable tumor or serum marker of malignant EOC due to its promotion of EOC cell invasion [39-41]. Finally, S100A4 regulates EMT and cancer metastasis, and S100A4 expression correlates with poor patient survival rates in several cancers [42]. S100A4 promotes EOC cell invasion via RhoA signaling, and nuclear expression of S100A4 is associated with aggressive cell behaviors and poor overall survival rates in EOCs [43]. Together, these findings suggest that CASZ1 modulates the expression of several key cytokines, chemokines, and metastasis-associated genes in EOC cells, thereby promoting EMT, invasion/metastasis, tumor growth and cancer immunosuppression.

Human CASZ1 is predominantly expressed as 2 alternatively spliced isoforms: CASZ1a and CASZ1b [6]. In this study, CASZ1a and CASZ1b were co-expressed in EOC tissues and exerted similar inhibitory effects on cell migration and invasion. The expression patterns of CASZ1a and CASZ1b were similar in EOC cell lines, but differed slightly in tumor tissues derived from EOC patients; CASZ1a mRNA expression was more frequently and strongly up-regulated in EOC tissues compared with CASZ1b. The discrepancy between CASZ1a and CASZ1b expression might result from distinct modes of post-transcriptional regulation via the various microRNAs predicted to target the 3'UTR of CASZ1a and CASZ1b. However, CASZ1a and CASZ1b share the same promoter [12]. Using the bioinformatics software TargetScan to identify microRNAs that potentially target CASZ1a and CASZ1b, we identified a conserved miR-142-3p binding sequence in the 3'UTR of CASZ1a, and conserved miR-146a and miR-146b-5p binding sequences were identified in the 3'UTR of CASZ1b. The existence of an IL-6/miR142-3p regulatory feedback-loop has been previously reported; IL-6 suppresses miR-142-3p expression, whereas IL-6 is a target of miR-142-3p [44]. Based on the decreased expression of IL-6 in CASZ1-knockdown MCAS cells, a CASZ1a/IL-6/miR142-3p regulatory feedback loop might be involved in EOC progression. However, the transcriptional and post-transcriptional regulation of CASZ1a and CASZ1b

expression in EOC requires further investigation.

In conclusion, our data indicate that CASZ1 is a novel promoter of metastasis in EOC. CASZ1 expression was up-regulated in EOC cells and tissues, with the strongest up-regulation observed in metastatic tumor tissues. In the future, the identification of CASZ1 downstream target genes will provide insight into the mechanism of metastasis in EOC and facilitate the development a novel therapeutic strategy for malignant ovarian cancer.

Acknowledgements

Disclosure of conflict of interest

None.

Address correspondence to: Dr. Keng-Fu Hsu, Department of Obstetrics and Gynecology, National Cheng Kung University Hospital, College of Medicine, National Cheng Kung University, Tainan, Taiwan. E-mail: d5580@mail.ncku.edu.tw

References

[1] Benedet JL, Bender H, Jones H 3rd, Ngan HY and Pecorelli S. FIGO staging classifications and clinical practice guidelines in the management of gynecologic cancers. FIGO Committee on Gynecologic Oncology. Int J Gynaecol Obstet 2000; 70: 209-262.

[2] Siegel R, Ma J, Zou Z and Jemal A. Cancer statistics, 2014. CA Cancer J Clin 2014; 64: 9-29.

[3] Clarke-Pearson DL. Clinical practice. Screening for ovarian cancer. N Engl J Med 2009; 361: 170-177.

[4] Lengyel E. Ovarian cancer development and metastasis. Am J Pathol 2010; 177: 1053-1064.

[5] Liu Z, Yang X, Tan F, Cullion K and Thiele CJ. Molecular cloning and characterization of human Castor, a novel human gene upregulated during cell differentiation. Biochem Biophys Res Commun 2006; 344: 834-844.

[6] Hitier R, Chaminade M and Preat T. The Drosophila castor gene is involved in postembryonic brain development. Mech Dev 2001; 103: 3-11.

[7] Mellerick DM, Kassis JA, Zhang SD and Odenwald WF. castor encodes a novel zinc finger protein required for the development of a subset of CNS neurons in Drosophila. Neuron 1992; 9: 789-803.

[8] Christine KS and Conlon FL. Vertebrate CASTOR is required for differentiation of cardiac precursor cells at the ventral midline. Dev Cell 2008; 14: 616-623.

[9] Vacalla CM and Theil T. Cst, a novel mouse gene related to Drosophila Castor, exhibits dynamic expression patterns during neurogenesis and heart development. Mech Dev 2002; 118: 265-268.

[10] Liu Z, Li W, Ma X, Ding N, Spallotta F, Southon E, Tessarollo L, Gaetano C, Mukouyama YS and Thiele CJ. Essential role of the zinc finger transcription factor Casz1 for mammalian cardiac morphogenesis and development. J Biol Chem 2014; 289: 29801-29816.

[11] Charpentier MS, Christine KS, Amin NM, Dorr KM, Kushner EJ, Bautch VL, Taylor JM and Conlon FL. CASZ1 promotes vascular assembly and morphogenesis through the direct regulation of an EGFL7/RhoA-mediated pathway. Dev Cell 2013; 25: 132-143.

[12] Liu Z, Naranjo A and Thiele CJ. CASZ1b, the short isoform of CASZ1 gene, coexpresses with CASZ1a during neurogenesis and suppresses neuroblastoma cell growth. PLoS One 2011; 6: e18557.

[13] Liu Z, Yang X, Li Z, McMahon C, Sizer C, Barenboim-Stapleton L, Bliskovsky V, Mock B, Ried T, London WB, Maris J, Khan J and Thiele CJ. CASZ1, a candidate tumor-suppressor gene, suppresses neuroblastoma tumor growth through reprogramming gene expression. Cell Death Differ 2011; 18: 1174-1183.

[14] Maines-Bandiera SL, Kruk PA and Auersperg N. Simian virus 40-transformed human ovarian surface epithelial cells escape normal growth controls but retain morphogenetic responses to extracellular matrix. Am J Obstet Gynecol 1992; 167: 729-735.

[15] Wu YH, Chang TH, Huang YF, Huang HD and Chou CY. COL11A1 promotes tumor progression and predicts poor clinical outcome in ovarian cancer. Oncogene 2014; 33: 3432-3440.

[16] Bagchi A and Mills AA. The quest for the 1p36 tumor suppressor. Cancer Res 2008; 68: 2551-2556.

[17] Dorr KM, Amin NM, Kuchenbrod LM, Labiner H, Charpentier MS, Pevny LH, Wessels A and Conlon FL. Casz1 is required for cardiomyocyte G1-to-S phase progression during mammalian cardiac development. Development 2015; 142: 2037-2047.

[18] Dijkgraaf EM, Welters MJ, Nortier JW, van der Burg SH and Kroep JR. Interleukin-6/interleukin-6 receptor pathway as a new therapy target in epithelial ovarian cancer. Curr Pharm Des 2012; 18: 3816-3827.

[19] Coward J, Kulbe H, Chakravarty P, Leader D, Vassileva V, Leinster DA, Thompson R, Schioppa T, Nemeth J, Vermeulen J, Singh N, Avril N, Cummings J, Rexhepaj E, Jirstrom K, Gallagher WM, Brennan DJ, McNeish IA and Balkwill FR. Interleukin-6 as a therapeutic target in human ovarian cancer. Clin Cancer Res 2011; 17: 6083-6096.

[20] Lane D, Matte I, Rancourt C and Piche A. Prognostic significance of IL-6 and IL-8 ascites levels in ovarian cancer patients. BMC Cancer 2011; 11: 210.

[21] Dobrzycka B, Mackowiak-Matejczyk B, Terlikowska KM, Kulesza-Bronczyk B, Kinalski M and Terlikowski SJ. Serum levels of IL-6, IL-8 and CRP as prognostic factors in epithelial ovarian cancer. Eur Cytokine Netw 2013; 24: 106-113.

[22] Nilsson MB, Langley RR and Fidler IJ. Interleukin-6, secreted by human ovarian carcinoma cells, is a potent proangiogenic cytokine. Cancer Res 2005; 65: 10794-10800.

[23] Wang Y, Li L, Guo X, Jin X, Sun W, Zhang X and Xu RC. Interleukin-6 signaling regulates anchorage-independent growth, proliferation, adhesion and invasion in human ovarian cancer cells. Cytokine 2012; 59: 228-236.

[24] Oh K, Moon HG, Lee DS and Yoo YB. Tissue transglutaminase-interleukin-6 axis facilitates peritoneal tumor spreading and metastasis of human ovarian cancer cells. Lab Anim Res 2015; 31: 188-197.

[25] Yin J, Zeng F, Wu N, Kang K, Yang Z and Yang H. Interleukin-8 promotes human ovarian cancer cell migration by epithelial-mesenchymal transition induction in vitro. Clin Transl Oncol 2015; 17: 365-370.

[26] Wang Y, Xu RC, Zhang XL, Niu XL, Qu Y, Li LZ and Meng XY. Interleukin-8 secretion by ovarian cancer cells increases anchorage-independent growth, proliferation, angiogenic potential, adhesion and invasion. Cytokine 2012; 59: 145-155.

[27] Merritt WM, Lin YG, Spannuth WA, Fletcher MS, Kamat AA, Han LY, Landen CN, Jennings N, De Geest K, Langley RR, Villares G, Sanguino A, Lutgendorf SK, Lopez-Berestein G, Bar-Eli MM and Sood AK. Effect of interleukin-8 gene silencing with liposome-encapsulated small interfering RNA on ovarian cancer cell

growth. J Natl Cancer Inst 2008; 100: 359-372.

[28] Kassim SK, El-Salahy EM, Fayed ST, Helal SA, Helal T, Azzam Eel D and Khalifa A. Vascular endothelial growth factor and interleukin-8 are associated with poor prognosis in epithelial ovarian cancer patients. Clin Biochem 2004; 37: 363-369.

[29] Xu L and Fidler IJ. Interleukin 8: an autocrine growth factor for human ovarian cancer. Oncol Res 2000; 12: 97-106.

[30] Kolomeyevskaya N, Eng KH, Khan AN, Grzankowski KS, Singel KL, Moysich K and Segal BH. Cytokine profiling of ascites at primary surgery identifies an interaction of tumor necrosis factor-alpha and interleukin-6 in predicting reduced progression-free survival in epithelial ovarian cancer. Gynecol Oncol 2015; 138: 352-357.

[31] Latha TS, Panati K, Gowd DS, Reddy MC and Lomada D. Ovarian cancer biology and immunotherapy. Int Rev Immunol 2014; 33: 428-440.

[32] Son DS, Parl AK, Rice VM and Khabele D. Keratinocyte chemoattractant (KC)/human growth-regulated oncogene (GRO) chemokines and pro-inflammatory chemokine networks in mouse and human ovarian epithelial cancer cells. Cancer Biol Ther 2007; 6: 1302-1312.

[33] De Filippo K, Dudeck A, Hasenberg M, Nye E, van Rooijen N, Hartmann K, Gunzer M, Roers A and Hogg N. Mast cell and macrophage chemokines CXCL1/CXCL2 control the early stage of neutrophil recruitment during tissue inflammation. Blood 2013; 121: 4930-4937.

[34] Kavandi L, Collier MA, Nguyen H and Syed V. Progesterone and calcitriol attenuate inflammatory cytokines CXCL1 and CXCL2 in ovarian and endometrial cancer cells. J Cell Biochem 2012; 113: 3143-3152.

[35] Liu J, Zhang N, Li Q, Zhang W, Ke F, Leng Q, Wang H, Chen J and Wang H. Tumor-associated macrophages recruit CCR6+ regulatory T cells and promote the development of colorectal cancer via enhancing CCL20 production in mice. PLoS One 2011; 6: e19495.

[36] Moshkovskii SA. Why do cancer cells produce serum amyloid A acute-phase protein? Biochemistry (Mosc) 2012; 77: 339-341.

[37] Edgell T, Martin-Roussety G, Barker G, Autelitano DJ, Allen D, Grant P and Rice GE. Phase II biomarker trial of a multimarker diagnostic for ovarian cancer. J Cancer Res Clin Oncol 2010; 136: 1079-1088.

[38] Urieli-Shoval S, Finci-Yeheskel Z, Dishon S, Galinsky D, Linke RP, Ariel I, Levin M, Ben-Shachar I and Prus D. Expression of serum amyloid a in human ovarian epithelial tumors: implication for a role in ovarian tumorigenesis. J Histochem Cytochem 2010; 58: 1015-1023.

[39] Acar A, Onan A, Coskun U, Uner A, Bagriacik U, Atalay F, Unsal DK and Guner H. Clinical significance of serum MMP-2 and MMP-7 in patients with ovarian cancer. Med Oncol 2008; 25: 279-283.

[40] Tanimoto H, Underwood LJ, Shigemasa K, Parmley TH, Wang Y, Yan Y, Clarke J and O'Brien TJ. The matrix metalloprotease pump-1 (MMP-7, Matrilysin): A candidate marker/target for ovarian cancer detection and treatment. Tumour Biol 1999; 20: 88-98.

[41] Wang FQ, So J, Reierstad S and Fishman DA. Matrilysin (MMP-7) promotes invasion of ovarian cancer cells by activation of progelatinase. Int J Cancer 2005; 114: 19-31.

[42] Boye K and Maelandsmo GM. S100A4 and metastasis: a small actor playing many roles. Am J Pathol 2010; 176: 528-535.

[43] Kikuchi N, Horiuchi A, Osada R, Imai T, Wang C, Chen X and Konishi I. Nuclear expression of S100A4 is associated with aggressive behavior of epithelial ovarian carcinoma: an important autocrine/paracrine factor in tumor progression. Cancer Sci 2006; 97: 1061-1069.

[44] Chiou GY, Chien CS, Wang ML, Chen MT, Yang YP, Yu YL, Chien Y, Chang YC, Shen CC, Chio CC, Lu KH, Ma HI, Chen KH, Liu DM, Miller SA, Chen YW, Huang PI, Shih YH, Hung MC and Chiou SH. Epigenetic regulation of the miR142-3p/interleukin-6 circuit in glioblastoma. Mol Cell 2013; 52: 693-706.

Supplementary Table 1. Top 10 up-and down-regulated genes and other metastasis-related genes in MCAS cells with sh-CASZ1 (2) and sh-CASZ1 (3), compared to that in sh-luc cells by the analysis of microarray data

| Gene symbol	Accession No.	Gene description	Log2 fold-change (sh-CASZ1 (2)/ sh-luc)	Log2 fold-change (sh-CASZ1 (3)/ sh-luc)
IL8	NM_000584.2	Homo sapiens interleukin 8	-2.97	-2.84
SERPINA3	NM_001085.4	Homo sapiens serpin peptidase inhibitor, clade A, member 3	-2.32	-2.19
GDF15	NM_004864.1	Homo sapiens growth differentiation factor 15	-2.22	-2.39
CXCL2	NM_002089.3	Homo sapiens chemokine (C-X-C motif) ligand 2	-2.12	-2.10
SAA1	NM_000331.3	Homo sapiens serum amyloid A1	-2.10	-1.98
CXCL1	NM_001511.1	Homo sapiens chemokine (C-X-C motif) ligand 1	-2.10	-2.13
C15ORF48	NM_032413.2	Homo sapiens chromosome 15 open reading frame 48	-2.05	-2.12
FST	NM_006350.2	Homo sapiens follistatin	-1.92	-1.96
PHGDH	NM_006623.2	Homo sapiens phosphoglycerate dehydrogenase	-1.85	-1.76
RARRES3	NM_004585.3	Homo sapiens retinoic acid receptor responder 3	-1.84	-1.78
CCL20	NM_004591.1	Homo sapiens chemokine (C-C motif) ligand 20	-1.76	-1.82
TNF	NM_000594.2	Homo sapiens tumor necrosis factor	-1.24	-1.33
MMP7	NM_002423.3	Homo sapiens matrix metallopeptidase 7	-1.05	-1.05
SAA4	NM_006512.1	Homo sapiens serum amyloid A4	-0.78	-0.82
IL6	NM_000600.1	Homo sapiens interleukin 6	-0.72	-0.80
S100A4	NM_019554.2	Homo sapiens S100 calcium binding protein A4	-0.68	-0.74
SAA2	NM_030754.2	Homo sapiens serum amyloid A2	-0.62	-0.59
DHRS9	NM_005771.3	Homo sapiens dehydrogenase/reductase member 9	1.41	1.41
SNAPC4	NM_003086.2	Homo sapiens small nuclear RNA activating complex, polypeptide 4	1.43	1.49
INTS1	NM_001080453.1	Homo sapiens integrator complex subunit 1	1.45	1.11
NTSR1	NM_002531.2	Homo sapiens neurotensin receptor 1	1.49	1.48
IL1RL1	NM_016232.4	Homo sapiens interleukin 1 receptor-like 1	1.60	1.53
TXNIP	NM_006472.2	Homo sapiens thioredoxin interacting protein	1.63	1.65
ZDHHC11	NM_024786.1	Homo sapiens zinc finger, DHHC-type containing 11	1.75	1.66
HAS3	NM_005329.2	Homo sapiens hyaluronan synthase 3	1.80	1.72
KRT6A	NM_005554.3	Homo sapiens keratin 6A	1.89	1.92
MMP1	NM_002421.2	Homo sapiens matrix metallopeptidase 1	2.03	2.13
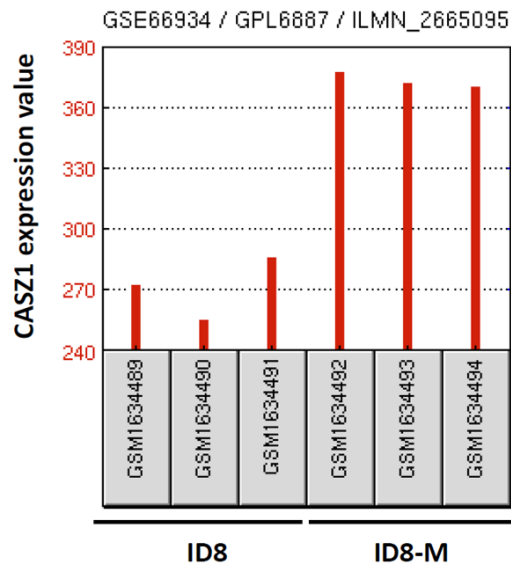
Supplementary Figure 1. CASZ1 expression is higher in mouse ovarian cancer cells with accelerated metastatic phenotype. CASZ1 expression is analyzed in a GEO dataset, GSE66934. ID8-M cells is *in vivo* selected from ascites in mice intraperitoneally injected parental ID8 cells, a mouse ovarian epithelial papillary serous adenocarcinoma cell line. ID8-M exhibits a rapid metastatic phenotype.

1
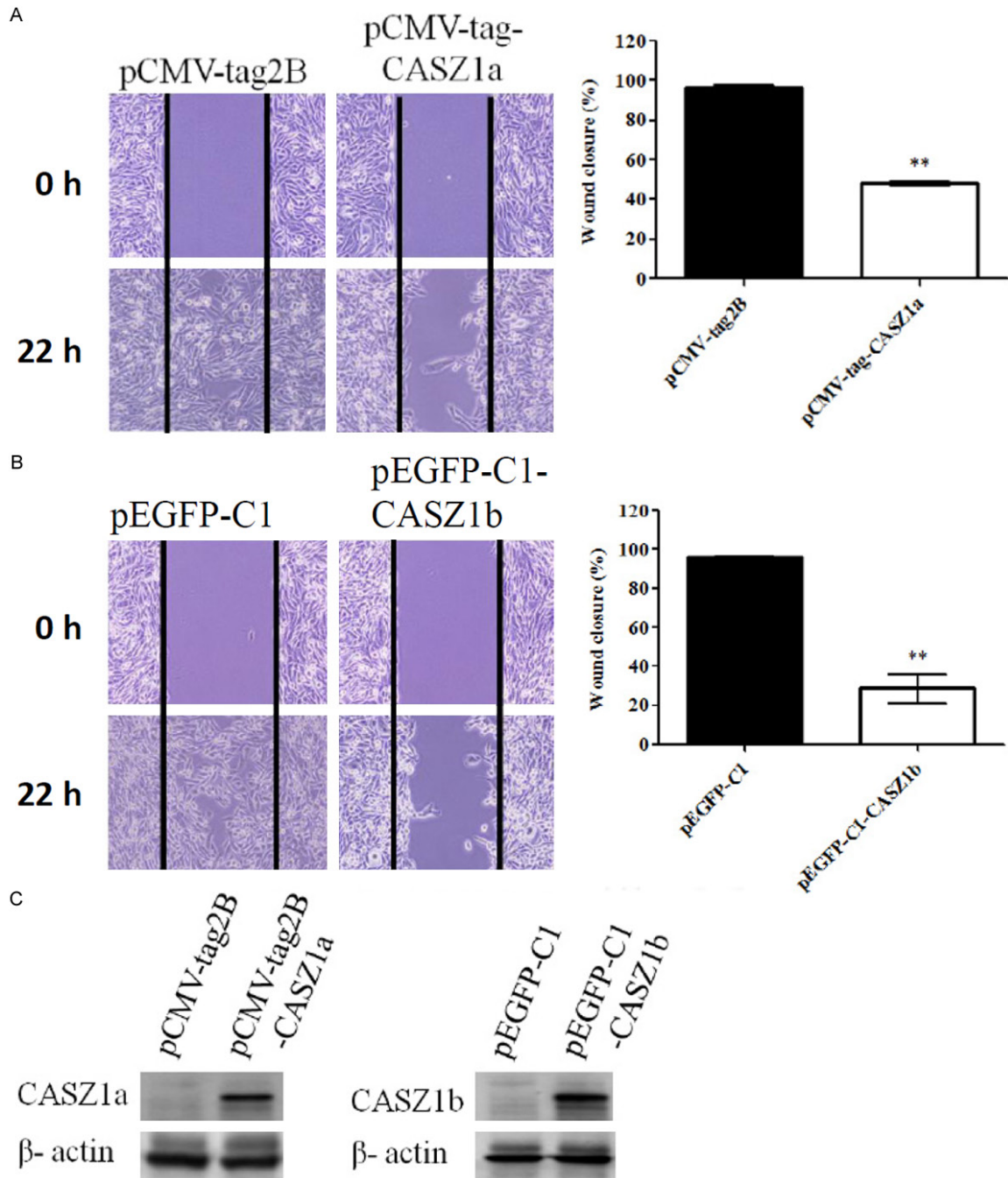
Supplementary Figure 2. Overexpression of CASZ1 inhibits the migration abilities in SHSY5Y cells. SH-SY5Y cells were transfected with pCMV-tag2B vector or pCMA-tag-CASZ1a (A), and pEGFP-C1 vector or pEGFP-C1-CASZ1b (B). The migration ability was examined by wound healing assay. Error bars represent SEM. **, P < 0.005 by Student's t-test. (C) The expression of CASZ1a or CASZ1b in CASZ1-overexpressed SH-SY5Y cells was analyzed by immunoblotting. β-actin was used as the internal control.
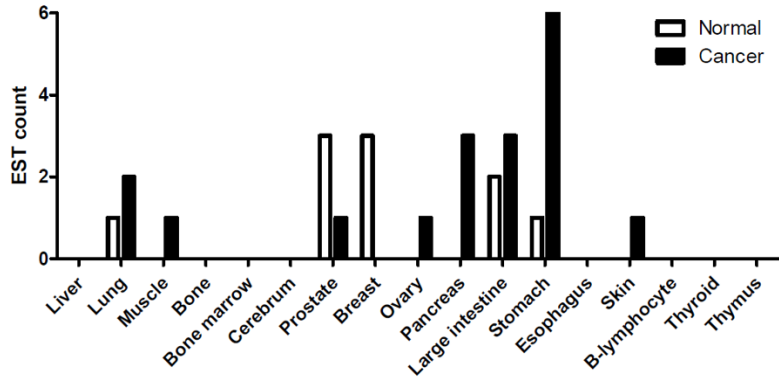
Supplementary Figure 3. CASZ1 is highly expressed in ovarian cancer tissues analyzed by *in silico* data mining. The EST expression analysis of the CASZ1 gene in different normal and cancerous tissues was modified from the ECgene database (http://genome.ewha.ac.kr/ECgene/).
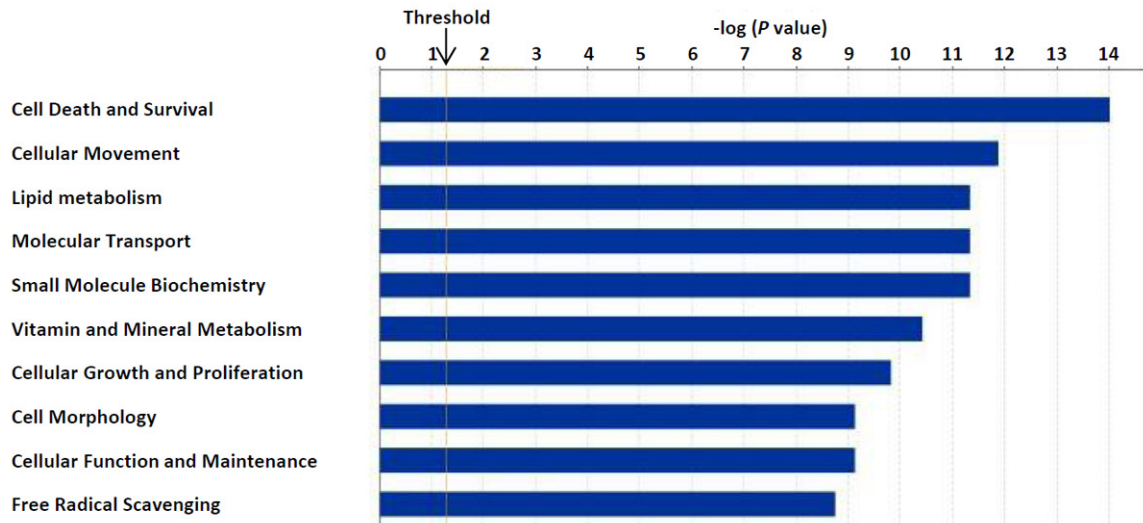
Supplementary Figure 4. Ingenuity Pathways Analysis (IPA) for microarray data of MCAS cells with sh-luc, sh-CASZ1 (2), and sh-CASZ1 (3).